OPTOELECTRONICS AND ADVANCED MATERIALS – RAPID COMMUNICATIONS Vol. 2, No. 12, December 2008, p. 792 - 795

Highly conducting and transparent multilayer films based on ZnO and Mo-doped indium oxide for optoelectronic applications

R. K. GUPTA*, K. GHOSH, R. PATEL[a], P. K. KAHOL
Department of Physics, Astronomy and Materials Science, Missouri State University, Springfield, MO-65897, USA
[a]Roy Blunt Jordan Valley Innovation Center, Missouri State University, Springfield, MO-65806, USA

Highly conducting and transparent multilayer films based on zinc oxide/molybdenum- doped indium oxide/zinc oxide (ZnO/IMO/ZnO) were deposited on quartz substrate by pulsed laser deposition technique. The effect of ZnO and IMO thickness on structural, optical, and electrical properties is studied. It is observed that these films are highly oriented along (002) and (222) direction for ZnO and IMO films respectively. The transparency of multilayer films is over 86%. The bandgap of these films depends on thickness of different layers and is in range of 3.20 eV-3.63 eV. The low resistivity (5.70×10^{-5} Ω.cm), high carrier concentration (4.53×10^{20} cm^{-3}), high mobility (242 $cm^2V^{-1}s^{-1}$), and wide bandgap make these multilayers suitable of optoelectronic applications.

(Received November 10, 2008; accepted November 27, 2008)

Keywords: Zinc oxide, Pulsed laser, Semiconductor, Optical property, Multilayer

1. Introduction

Thin films of transparent conducting oxides are widely used for optoelectronic applications. They are widely used for flat panel display, organic light emitting diodes and photovoltaic applications [1,2,3]. Among these, zinc oxide and indium oxide based materials are most popular for these applications [4,5]. Recently, metal oxide/metal/metal oxide sandwich structures have attracted considerable attention because of their good transparency and low resistivity [6,7]. These meal oxide/metal/metal oxide multilayer are used as highly conducting and transparent electrodes for flat panel display and transparent heat mirrors for energy conserving windows [8]. .

Different techniques such as sputtering [9], rf plasma-assisted laser ablation [10], chemical vapor deposition [11], vacuum thermal evaporation [12], ion-beam sputtering [13], and pulsed laser deposition [14] have been used for deposition of multilayer transparent conducting electrodes. Recently multilayer systems based on semiconductor (ZnO) and metals (Ag, Cu, and Al) are used to improve the properties of ZnO films [15,16,17]. But the problem with metal as a middle layer is that, it reduces the transparency of the metal oxide and also the mobility of these films is not very high [18]. In this communication, we report the effect of thickness of middle layer on structural, optical and electrical properties of ZnO films. Molybdenum-doped indium oxide (IMO) is used as a middle layer. We chose IMO as a middle layer because of to its low electrical resistivity, high electron mobility and high transparency [19].

2. Experimental details

ZnO and IMO targets for the pulsed laser deposition were prepared by the standard solid-state reaction method using high purity of ZnO, In_2O_3 and MoO_3. For IMO target, required amounts of In_2O_3 and MoO_3 were taken by molecular weight to get two atomic weight percent of molybdenum. The well-ground mixture was heated at 800 ˚C for 12 hours. The powder mixture was cold pressed at 6×10^6 N/m^2 load and sintered at 850 ˚C for 12 hours.

ZnO, IMO and multilayer of ZnO/IMO/ZnO were deposited on quartz using KrF excimer laser (Lambda Physik COMPex, λ = 248 nm and pulsed duration of 20 ns). The laser was operated at a pulse rate of 10 Hz, with an energy of 300 mJ/pulse. The laser beam was focused onto a rotating target at a 45˚ angle of incidence. The multilayers of ZnO/IMO/ZnO were deposited at 500 ˚C under oxygen pressure of 1.0×10^{-3} mbar. The deposition chamber was initially evacuated to 1.2×10^{-6} mbar and then oxygen gas was introduced into the chamber during deposition. The growth rate for the films was ~3 nm/min.

The structural characterizations were performed using x-ray diffraction (XRD) and atomic force microscopy (AFM). The XRD spectra of all the films were recorded with Bruker AXS x-ray diffractometer using the 2θ-θ scan with CuK_α (λ = 1.5405Å) radiation which operated at 40 kV and 40 mA. The AFM imaging was performed under ambient conditions using a Digital Instruments (Veeco) Dimension-3100 unit with Nanoscope® III controller, operating in tapping mode. The optical transmittance measurements were made using UV-visible spectrophotometer (Ocean Optics HR4000).

The resistivity and Hall coefficient measurements were carried out by a standard four-probe technique. The Hall effect was measured with the magnetic field applied perpendicular to film surface in the Van der Pauw configuration [20]. Carrier concentration and carrier mobility were calculated at room temperature using Hall coefficient and resistivity data [21].

3. Results and discussion

3.1. Structural characterization

Structural characterization of these films is done using x-ray diffraction and atomic force microscopy. Fig. 1 shows the x-ray diffraction patterns of ZnO, IMO and ZnO/IMO/ZnO multilayer of different thicknesses. It is observed that all the films are highly oriented. It is seen that ZnO films are highly oriented along (002) direction and IMO films are oriented along (222) direction. The average particle size (t) of the films was calculated using the Scherrer equation, $t = 0.9\lambda/\beta\cos\theta$, where λ is the x-ray wavelength, β is the full width at half maximum of diffraction line, and $\theta$is the diffraction angle of the XRD spectra [22]. The average particle size of ZnO and IMO is 18.1 nm and 15.3 nm respectively.

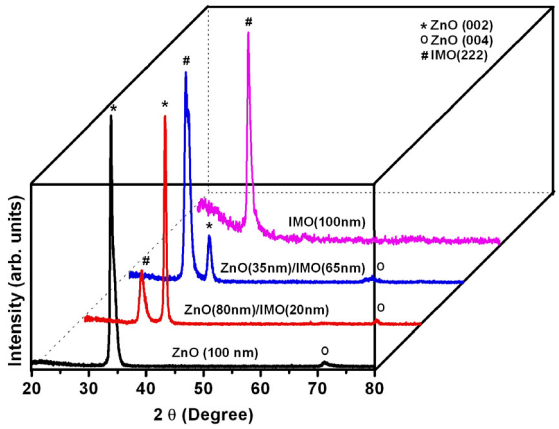

Fig. 1. XRD patterns of ZnO/IMO/ZnO films.

The atomic force microscopy images of ZnO, IMO and their multilayer are shown in Fig. 2 The scan was carried out in tapping mode. The spring constant of the cantilever was ~42 N/m. The cantilevered tip was oscillated close to the mechanical resonance frequency of the cantilever (typically, 200-300 kHz) with amplitudes ranging from ~10 to 30 nm. It is observed that all the films have very smooth surfaces. The root mean square values of surface roughness of all the films are in range of 1.1-2.2 nm. It is seen that multilayer films have improved surface roughness compared to pure ZnO film. But for any device fabrication, not only root mean square surface roughness but also peak to valley roughness is important. It is reported that the leakage current of the device increases with an increase in the peak to valley roughness [23]. The peak to valley roughness of all the multilayer films is in range of 11-15 nm. For devices based on tin doped indium oxide the peak to valley roughness is reported as 16.4 nm.

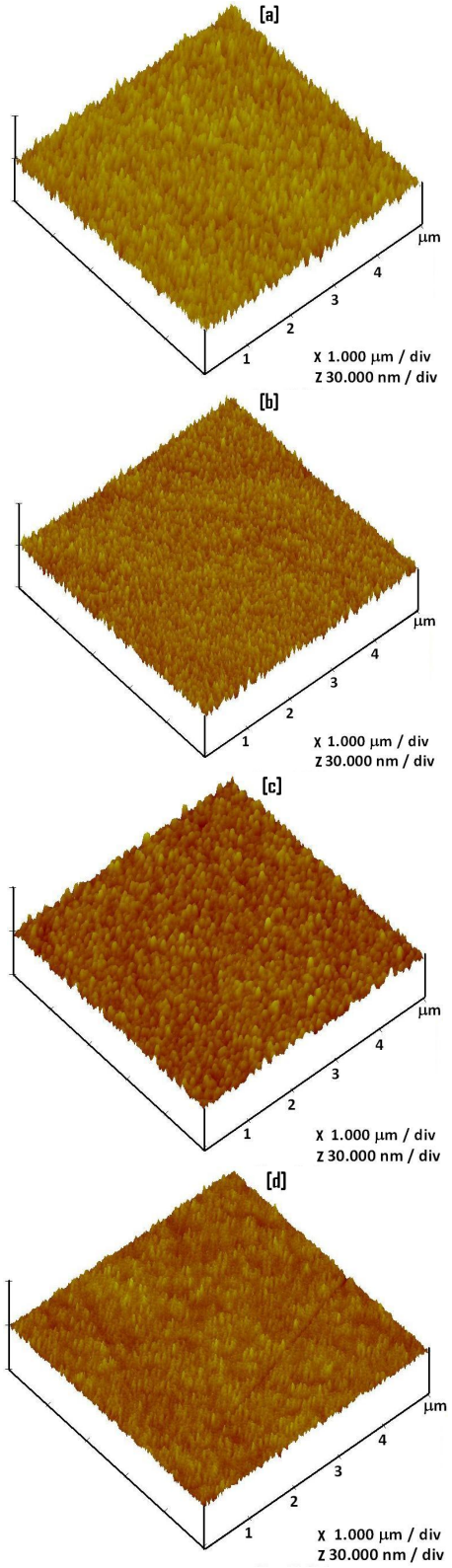

Fig. 2. AFM images of (a) ZnO (100 nm), (b) IMO (100 nm), (c) ZnO (80 nm)/IMO (20 nm), and (d) ZnO (35 nm)/IMO (65 nm) films.

3.2. Optical characterization

The optical characterization of these films is done using uv-visible spectroscopy. The optical transmission spectrum of pure ZnO, IMO and multilayer were measured in the range of 350 nm-950 nm and shown in Fig. 3(a). It is observed that all the films have very high transmittance in the visible range of solar spectrum. Ramachandran et al. have deposited ZnO/Pt/ZnO multilayer and observed decrease in transmittance from ~ 60 % to ~ 25 % with increase in platinum layer thickness from 7 nm to 15 nm respectively [24]. The advantage of all oxide based multilayer films is that the transparency of films is very high and almost independent of middle layer thickness.

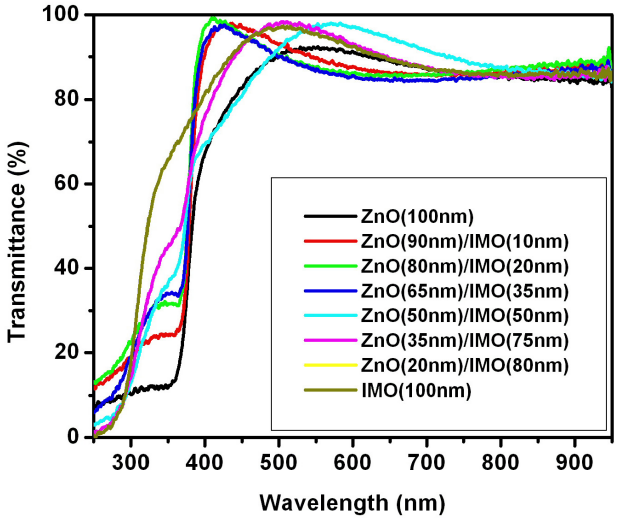

Fig. 3(a). Transmittance spectra of ZnO/IMO/ZnO films.

The optical band gap of these films is calculated from the transmittance versus wavelength spectra. The absorption coefficient (α) is calculated using the equation [25]

$$\alpha = \ln\left(\frac{1}{T}\right)/d$$

where T is transmittance and d is film thickness. The absorption coefficient (α) and the incident photon energy ($h\nu$) is related by the following equation [26]

$$(\alpha h\nu)^2 = A(h\nu - E_g)$$

where A and E_g are constant and optical band gap, respectively. The E_g can be determined by extrapolations of the linear portion of the curve to the $h\nu$ axis. The Fig. 3(b) shows the curves of $(\alpha h\nu)^2$ versus photon energy. The optical band gap is found varying between 3.20 and 3.63 eV for various films. The increase in band gap of ZnO films may be explained by the Burstein-Moss shift [27]. According to this, the increase in carrier concentration increases the absorption edge shifts towards higher energy. By making multilayer of ZnO and IMO, the carrier concentration of multilayer films increase with increase in thickness of IMO film. This increase in carrier concentration increases the optical bandgap.

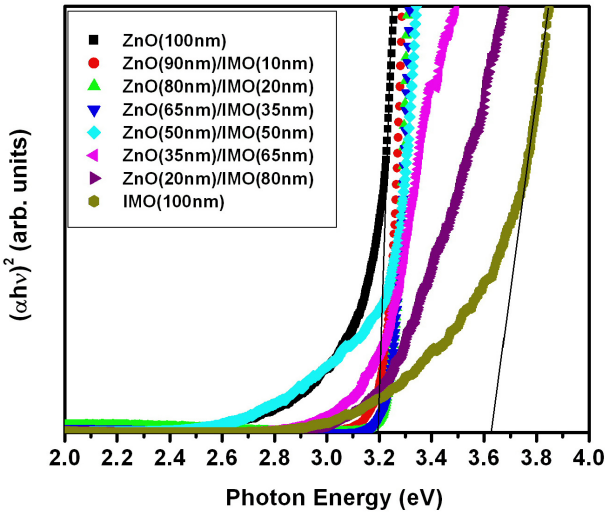

Fig. 3(b). Plot of $(\alpha h\nu)^2$ vs. $h\nu$ of ZnO/IMO/ZnO films.

3.3. Electrical characterization

The electrical properties such as resistivity, carrier concentration and mobility of the films are discussed next. The electrical resistivity of films was determined by taking the product of resistance and film thickness. The carrier concentration (n) is derived from the relation $n = 1/e.R_H$, where R_H is the Hall coefficient and e is the absolute value of the electron charge. The carrier mobility (μ) is determined using the relation $\mu = 1/ne\rho$, where ρ is resistivity. Fig. 4 shows the effect of IMO films thickness on electrical properties of ZnO/IMO/ZnO multilayer films. It is observed that the resistivity of the ZnO/IMO/ZnO multilayer films decreases with increase in thickness of IMO film. The electrical resistivity of pure ZnO films is 9.56×10^{-3} Ω.cm, which decreases to 5.70×10^{-5} Ω.cm for ZnO(10 nm)/IMO(80 nm)/ZnO(10 nm) multilayer. On the other hand, the carrier concentration and mobility is found to increase with increase in film thickness of IMO in multilayer. The electron mobility increases from 59 $cm^2V^{-1}s^{-1}$ to 242 $cm^2V^{-1}s^{-1}$ with increase in IMO film thickness from 0 nm to 80 nm respectively. The carrier concentration of ZnO film is 1.11×10^{19} cm^{-3}, which increases to 3.90×10^{20} cm^{-3}, and 4.53×10^{20} cm^{-3} with introduction of IMO film having thickness of 35 nm and 80 nm respectively.

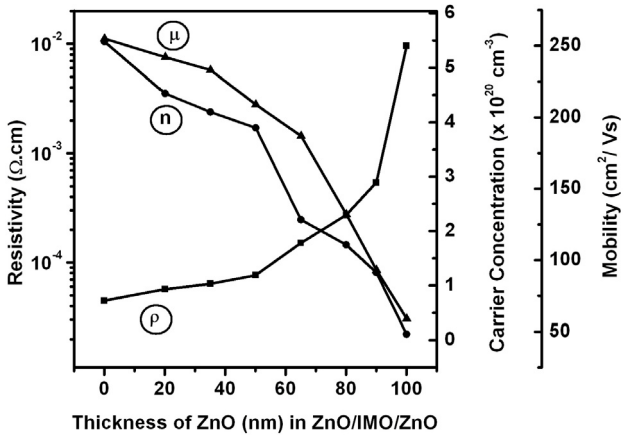

Fig. 4. Effect of IMO film thickness on resistivity (ρ), carrier concentration (n), and mobility (μ) of ZnO/IMO/ZnO films.

4. Conclusions

Pulsed laser deposition technique is used for deposition of ZnO, IMO and multilayer of ZnO/IMO/ZnO. These films are highly transparent (~ 86 %) in visible range with very smooth surface roughness. X- ray diffraction studies reveal that these films are highly oriented along (002) and (222) direction for ZnO and IMO respectively. The optical band gap is found varying between 3.20 and 3.63 eV for various films. The low resistivity (5.70×10^{-5} Ω.cm), high carrier concentration (4.53×10^{20} cm^{-3}), high mobility (242 $cm^2V^{-1}s^{-1}$), and wide bandgap make these multilayer suitable of optoelectronic applications.

Acknowledgements

RKG thankfully acknowledges Missouri State University for the Research Assistant Professor position. The authors wish to acknowledge Prof. R. Mayanovic, Missouri State University, for providing XRD facility.

References

[1] B. G. Lewis, D. C. Paine, MRS Bull. **25**, 22 (2000).
[2] H. Kim, C. M. Gilmore, A. Pique, J. S. Horwitz, H. Mattoussi, H. Murata, Z.H. Kafafi, D.B. Chrisey, J. Appl. Phys. **11**, 6451 (1999).
[3] J. A. A. Selvan, A. E. Delahoy, S. Guo, Y. M. Li, Sol. Energy Mater. Sol. Cells **90**, 3371 (2006).
[4] L. Zhao, J. Lian, Y. Liu, Q. Jiang, Appl. Surf. Sci. **252**, 8451 (2006).
[5] F. O. Adurodija, L. Semple, R. Bruning, Thin Solid Films **492**, 153 (2005).
[6] Y. S. Jung, Y. W. Choi, H. C. Lee, D. W. Lee, Thin Solid Films **440**, 278 (2003).
[7] S. Ramachandran, A. Chugh, A. Tiwari, J. Narayan, J. Cryst. Growth **291**, 212 (2006).
[8] M. Bender, W. Seelig, C. Daube, H. Frankenberger, B. Ocker, J. Stollenwerk, Thin Solid Films **326**, 67 (1998).
[9] K. Ellmer, G. Vollweiler, Thin Solid Films **496**, 104 (2006).
[10] B. Mitu, V. Marotta, S. Orlando, Appl. Surf. Sci. **252**, 4637 (2006).
[11] C. T. Lee, Q. X. Yu, B. T. Tang, H. Y. Lee, F. T. Hwang, Appl. Phys. Lett. **78**, 3412 (2001).
[12] H. Pang, Y. Yuan, Y. Zhou, J. Lian, L. Cao, J. Zhang, X. Zhou, J. Luminescence **122-123**, 587 (2007).
[13] Y. M. Hu, C. W. Lin, J. C. A. Huang, Thin Solid Films **497**, 130 (2006).
[14] E. J. J. Martin, M. Yan, M. Lane, J. Ireland, C. R. Kannewurf, R. P. H. Chang, Thin Solid Films **461**, 309 (2004).
[15] D. R. Sahu, S. Y. Lin, J. L. Huang, Appl. Surf. Sci. **252**, 7509 (2006).
[16] D. R. Sahu, J. L. Huang, Appl. Surf. Sci. **253**, 827 (2006).
[17] Y. M. Hu, C. W. Lin, J. C. A. Huang, Thin Solid Films **497**, 130 (2006).
[18] S. Ramachandran, A. Chugh, A. Tiwari, J. Narayan, J. Cryst. Growth **291**, 212 (2006).
[19] R. K. Gupta, K. Ghosh, S. R. Mishra, P. K. Kahol, Appl. Surf. Sci. **254**, 4018 (2008).
[20] L. J. Van der Pauw, Philips Res. Rep. **13**, 1 (1958).
[21] R. K. Gupta, K. Ghosh, S. R. Mishra, P. K. Kahol, Appl. Surf. Sci. **254**, 1661 (2008).
[22] V. Khranovskyy, U. Grossner, O. Nilsen, V. Lazorenko, G. V. Lashkarev, B. G. Svensson, R. Yakimova, Thin Solid Films **515**, 472 (2006).
[23] Y. H. Tak, K. B. Kim, H. G. Park, K. H. Lee, J. R. Lee, Thin Solid Films **411**, 12 (2002).
[24] S. Ramachandran, A. Chugh, A. Tiwari, J. Narayan, J. Cryst. Growth **291**, 212 (2006).
[25] W. Miao, X. Li, Q. Zhang, L. Huang, Z. Zhang, L. Zhang, X. Yan, Thin Solid Films **500**, 70 (2006).
[26] V. R. Shinde, T. P. Gujar, C. D. Lokhande, R. S. Mane, S. H. Han, Mater. Chem. Phys. **96**, 326 (2006).
[27] S. M. Park, T. Ikegami, K. Ebihara, P. K. Shin, Appl. Surf. Sci. **253**, 1522 (2006).

*Corresponding author: ramguptamsu@gmail.com